



Enhanced dielectric nonlinearity in epitaxial $\text{Pb}_{0.92}\text{La}_{0.08}\text{Zr}_{0.52}\text{Ti}_{0.48}\text{O}_3$ thin films

Chunrui Ma, Beihai Ma, Shao-Bo Mi, Ming Liu, and Judy Wu

Citation: *Applied Physics Letters* **104**, 162902 (2014); doi: 10.1063/1.4872375

View online: <http://dx.doi.org/10.1063/1.4872375>

View Table of Contents: <http://scitation.aip.org/content/aip/journal/apl/104/16?ver=pdfcov>

Published by the [AIP Publishing](#)

Articles you may be interested in

[Temperature-dependent dielectric nonlinearity of relaxor ferroelectric \$\text{Pb}_{0.92}\text{La}_{0.08}\text{Zr}_{0.52}\text{Ti}_{0.48}\text{O}_3\$ thin films](#)

Appl. Phys. Lett. **102**, 202901 (2013); 10.1063/1.4807665

[Temperature dependent polarization switching properties of ferroelectric \$\text{Pb}_{0.92}\text{La}_{0.08}\text{Zr}_{0.52}\text{Ti}_{0.48}\text{O}_3\$ films grown on nickel foils](#)

Appl. Phys. Lett. **102**, 072901 (2013); 10.1063/1.4793304

[Estimation of intrinsic contribution to dielectric response of \$\text{Pb}_{0.92}\text{La}_{0.08}\text{Zr}_{0.52}\text{Ti}_{0.48}\text{O}_3\$ thin films at low frequencies using high bias fields](#)

Appl. Phys. Lett. **102**, 062906 (2013); 10.1063/1.4792529

[Enhanced dielectric properties of \$\text{Pb}_{0.92}\text{La}_{0.08}\text{Zr}_{0.52}\text{Ti}_{0.48}\text{O}_3\$ films with compressive stress](#)

J. Appl. Phys. **112**, 114117 (2012); 10.1063/1.4768926

[Role of dual-laser ablation in controlling the Pb depletion in epitaxial growth of \$\text{Pb}\(\text{Zr}_{0.52}\text{Ti}_{0.48}\)\text{O}_3\$ thin films with enhanced surface quality and ferroelectric properties](#)

J. Appl. Phys. **111**, 064102 (2012); 10.1063/1.3694035

The image shows the cover of an Applied Physics Reviews journal issue. It features a blue and orange color scheme with a molecular structure background. The text 'NEW Special Topic Sections' is prominently displayed in white. Below it, 'NOW ONLINE' is written in yellow, followed by the title 'Lithium Niobate Properties and Applications: Reviews of Emerging Trends' in white. The AIP Applied Physics Reviews logo is in the bottom right corner.

NEW Special Topic Sections

NOW ONLINE
Lithium Niobate Properties and Applications:
Reviews of Emerging Trends

AIP Applied Physics Reviews

Enhanced dielectric nonlinearity in epitaxial $\text{Pb}_{0.92}\text{La}_{0.08}\text{Zr}_{0.52}\text{Ti}_{0.48}\text{O}_3$ thin films

Chunrui Ma,^{1,a)} Beihai Ma,² Shao-Bo Mi,^{3,4} Ming Liu,³ and Judy Wu^{1,a)}

¹*Department of Physics and Astronomy, University of Kansas, Lawrence, Kansas, 66045, USA*

²*Energy Systems Division, Argonne National Laboratory, Argonne, Illinois 60439, USA*

³*Electronic Materials Research Laboratory, Key Laboratory of the Ministry of Education and International Center for Dielectric Research, Xi'an Jiaotong University, Xi'an 710049, China*

⁴*Shenyang National Laboratory for Materials Science, Institute of Metal Research, Chinese Academy of Sciences, Shenyang 110016, People's Republic of China*

(Received 7 March 2014; accepted 3 April 2014; published online 23 April 2014)

High quality c-axis oriented epitaxial $\text{Pb}_{0.92}\text{La}_{0.08}\text{Zr}_{0.52}\text{Ti}_{0.48}\text{O}_3$ films were fabricated using pulsed laser deposition on (001) LaAlO_3 substrates with conductive LaNiO_3 buffers. Besides confirmation of the in-plane and out-of-plane orientations using X-ray diffraction, transmission electron microscopy study has revealed columnar structure across the film thickness with column width around 100 nm. Characterization of ferroelectric properties was carried out in comparison with polycrystalline $\text{Pb}_{0.92}\text{La}_{0.08}\text{Zr}_{0.52}\text{Ti}_{0.48}\text{O}_3$ films to extract the effect of epitaxial growth. It is found that the ratio between the irreversible Rayleigh parameter and reversible parameter increased up to 0.028 cm/kV at 1 kHz on epitaxial samples, which is more than twice of that on their polycrystalline counterparts. While this ratio decreased to 0.022 cm/kV with increasing frequency to 100 kHz, a much less frequency dependence was observed as compared to the polycrystalline case. The epitaxial $\text{Pb}_{0.92}\text{La}_{0.08}\text{Zr}_{0.52}\text{Ti}_{0.48}\text{O}_3$ films exhibited a higher mobility of domain wall and the higher extrinsic contribution to the dielectric properties, as well as reduced density of defects, indicating that it is promising for tunable and low power consumption devices. © 2014 AIP Publishing LLC. [<http://dx.doi.org/10.1063/1.4872375>]

Research and development of ferroelectric films and devices have attracted much attention recently due to their potential applications on nonvolatile random access memories, energy storage capacitors, electro-mechanical, or photo-mechanical transducers, etc.^{1–3} Among them, Lead zirconate titanate system (PZT), which exhibits remarkable piezoelectric effect, high dielectric permittivity, and breakdown electric field, has been the focus of intensive research.^{3–5} In particular, $\text{Pb}(\text{Zr}_{0.52}\text{Ti}_{0.48})\text{O}_3$ with a low coercive field and high remnant polarization⁶ has been widely investigated for application in microwave devices,⁷ energy storage, and capacitance.⁸ However, the common Pb loss induced a large number of oxygen vacancies, which locate typically at grain boundaries or/and at the interfaces between PZT and electrodes. Recently, lanthanum doped PZT with different Zr/Ti ratio, such as 65/35, 53/47, or 20/80, has been investigated, since it can effectively reduce oxygen vacancy, decrease leakage current, and lower the fatigue and domain pinning.^{8–10} In general, higher La content makes the peaks of the dielectric permittivity broader and the temperature of the permittivity maxima T_m lower. For example, the T_m of La-doped PZT with a Zr/Ti ratio of 65/35 decreased from 350 °C to 105 °C with increasing La content from 0 to 8 at. %. Especially, $\text{Pb}_{0.92}\text{La}_{0.08}\text{Zr}_{0.52}\text{Ti}_{0.48}\text{O}_3$ [PLZT in the rest of this paper] is in the ferroelectric tetragonal region with suitable Curie temperature for application in hybrid electric vehicles. Polycrystalline films fabricated by chemical solution deposition exhibited a high energy storage

density of 22 J/cm³ and electric efficiency of 77%, demonstrating that it is promising for applications in capacitors for power electronic systems and energy storage.^{11–14} PLZT also is an interesting system for basic research of effect of defects on the intrinsic and extrinsic ferroelectric properties.¹⁵

Epitaxial PLZT films are ideal for such a study due to much reduced crystallographic defects, especially large-angle grain boundary. Moreover, employment of pulsed laser deposition (PLD) for epitaxial growth of PLZT films provides the benefit of reducing defects introduced during fabrication process such as residual fine pores, hydroxyls, and cracking during the drying stage in solution deposition processes. Motivated by this, we have explored epitaxial PLZT films fabrication by PLD. However, one substantial challenge is the balance between Pb loss and quality of PLZT film, since Pb is easy to loss when temperature exceeds ~650 °C,¹⁶ while the formation of high quality PLZT films require high temperature. Oxygen partial pressure can further complicate the growth process, since inadequate oxidation at temperatures above ~500 °C may result in oxygen vacancies and degraded sample properties. In particular, the pyrochlore phase can be eliminated when the temperature is higher than 500 °C at low oxygen partial pressure.¹⁷ Perovskite phase has been reported in a narrow range of oxygen pressure (200 mTorr < P_{O_2} < 300 mTorr).¹⁸ Thus, the temperature and oxygen pressure must be adjusted delicately to obtain highly epitaxial PLZT films. In this work, we report epitaxial growth of PLZT films by PLD, characterization of their dielectric and ferroelectric properties in comparison with those on polycrystalline PLZT samples.

^{a)}Authors to whom correspondence should be addressed. Electronic addresses: chunrui.ma@gmail.com and jwu@ku.edu.

(001) LaAlO_3 (LAO) substrates were employed for epitaxial growth of the conductive LaNiO_3 (LNO) layers (serve as the bottom electrodes) and PLZT films consecutively by PLD. Stoichiometric LNO target and 20 mol. % Pb-rich PLZT target to compensate for the Pb loss were used in this study. LNO is a good candidate as the bottom electrode for the ferroelectric capacitor and memory device due to its high conductivity, while its properties are sensitively affected by the growth conditions. Especially, a narrow window of the deposition temperature between 600°C to 700°C has been reported.¹⁹ Compositional change occurs above 700°C , while its mobility decreases considerably below 600°C . The optimal LNO conductivity is reported at the oxygen partial pressures 225 mTorr at 625°C . This condition also falls in the optimal growth window for PLZT; thus, it was selected for the growth of PLZT/LNO hetero-structures *in situ* on LAO substrate by using PLD with KrF excimer laser (wavelength of 248 nm and pulse width of 25 ns). The average laser pulse energy density was 2 J/cm^2 and repetition rate is 10 Hz. After finishing deposition, the deposition chamber was backfilled to 600 Torr oxygen and the films were *in situ* annealed at 625°C for 30 min to reduce oxygen vacancies in the films before cooling down to room temperature. Platinum top electrodes with thickness of 100 nm were deposited by electron-beam evaporation through a shadow mask to define $250\text{-}\mu\text{m}$ -diameter circular top electrodes. The microstructure, crystallinity, and epitaxial behavior of the PLZT films were systematically examined by X-ray diffraction (XRD) and transmission electron microscopy (TEM). A probe system was used for electrical characterization at room temperature.

Fig. 1(a) plotted a XRD θ - 2θ profile measured with a tilt angle at 45° with respect to the normal of the film. The three peaks correspond to the (110) peaks of PLZT, LNO, and LAO, respectively, indicating that the PLZT and LNO film is *c*-axis oriented. XRD pole figures were taken to evaluate the epitaxial quality and determine the interface relationship between the PLZT and LNO films on the LAO substrate. Figs. 1(b)–1(d) illustrated the (111) pole figures

for the PLZT, LNO, and LAO, respectively. The fourfold symmetry reflections with well defined sharp poles are clearly seen, indicating the PLZT films have an anticipated biaxial epitaxial relationship with the substrate: $(100)_{\text{PLZT}} // (100)_{\text{LNO}} // (100)_{\text{LAO}}$ and $(001)_{\text{PLZT}} // (001)_{\text{LNO}} // (001)_{\text{LAO}}$. The average full width at half maximum (FWHM) measured from the PLZT (111) ϕ -scan peaks is 1.34° . Based on the XRD data, the out-of-plane lattice constant of PLZT film is estimated to be 4.063 \AA , which is comparable to the lattice constant of the bulk PLZT material $c = 4.068 \pm 0.005\text{ \AA}$,²⁰ indicating that the interface strain induced by the lattice mismatch between LNO is most probably released at the film thickness of 500 nm through the formation of misfit dislocations and other defects. Fig. 1(e) is a cross sectional TEM image of PLZT/LNO/LAO hetero-structure, gold is deposited on the film to prevent the accumulation of charge at the film during the TEM study. It is interesting that the columnar structured growth dominates in the PLZT films and the columnar grains are mostly perpendicular to the substrate with typical column width of $\sim 100\text{ nm}$. Most grains span the full thickness of the film ($\sim 500\text{ nm}$), indicating that the uniformly polarized crystallites could be easily realized in it.^{21,22} The columnar structure seems to roughen its surface as shown in Fig. 1(e), which is consistent with the average surface roughness around 1.49 nm and 10 nm on LNO and PLZT, respectively, over an area of $1 \times 1\text{ }\mu\text{m}^2$ from atomic force microscopy measurement. This indicates that the surface of LNO is very flat as bottom electrode. The increased surface roughness observed on PLZT films is most probably associated to the strained epitaxial growth of PLZT on LNO.

Fig. 2(a) depicts the current density measured as a function of electrical field at 1 s after a pulsed DC electric field was applied across the PLZT films. It increases with the applied field from around $\sim 2 \times 10^{-8}\text{ A/cm}^2$ at 6 kV/cm to $\sim 3 \times 10^{-6}\text{ A/cm}^2$ at 128 kV/cm. The low leakage current density observed suggests that the PLZT films have high resistivity desired for applications. Fig. 2(b) shows the time relaxation current density measured after a constant applied field of 40 kV/cm was applied. The decay in dielectric

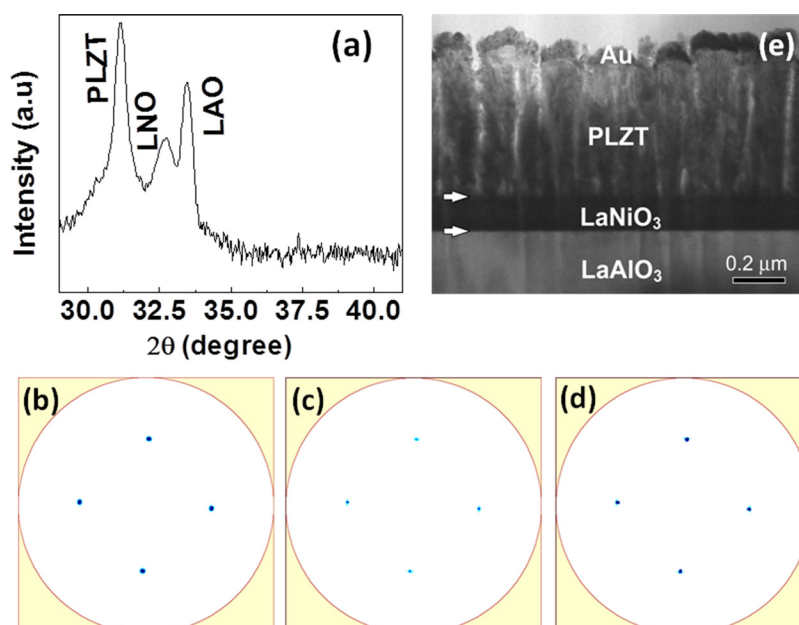


FIG. 1. (a) XRD profile of PLZT/LNO on LAO substrate measured with 45° tilt angle, (b) PLZT (111), (c) LNO (111), (d) LAO (111) pole figures, (e) cross sectional TEM image of PLZT/LNO/LAO.

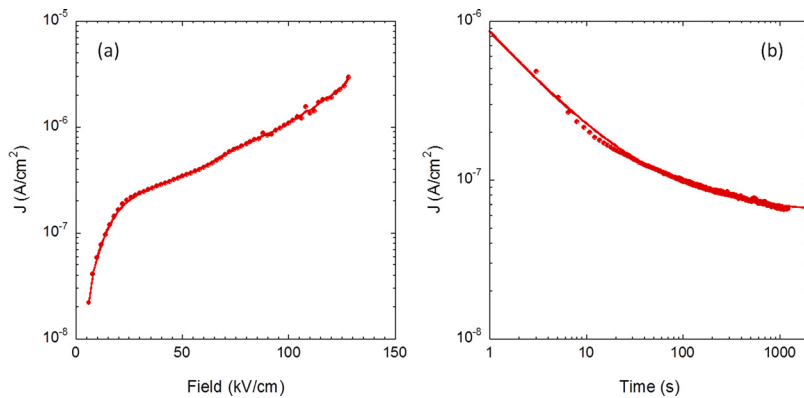


FIG. 2. (a) Field dependent current density. (b) Time relaxation current density of epitaxial PLZT film.

relaxation current obeys the Curie-von Schweidler law (solid line):²³ $J = J_s + J_0 \times t^{-n}$, where J_s is the steady-state current density, J_0 is a fitting constant, t is relaxation time in seconds, and n is the slope of the $\log J$ - $\log t$ plot. The steady state leakage current density $J_s = 6.2 \times 10^{-8}$ A/cm², which is a factor of three higher than 2×10^{-8} A/cm² in the polycrystalline PLZT film.²⁴ Normally, the polycrystalline films have a much higher resistivity as compared to their epitaxial counterparts because of much higher density of structural defects, especially grain boundaries, acting as trapping-scattering center for the free carriers, reducing their mobility in polycrystalline films.^{25,26}

An Agilent E4980A precision LCR Meter was used to determine the relative permittivity and dielectric loss of epitaxial PLZT film under an applied bias field. Under zero bias, the relative permittivity $\varepsilon(0)$ is up to 1225, which represents about 9% decrease from 1350 for polycrystalline PLZT films, as shown in Fig. 3(a).²⁴ This is not surprising since higher permittivity is expected in the latter due to the presence of grain boundaries, which bring an additional contribution to the polarization charges.²⁵ The dielectric loss in the epitaxial PLZT film is as low as 0.04, which is comparable to the lowest dielectric loss of 0.035 in polycrystalline PLZT thin film.²⁶ The relative permittivity and loss exhibit the butterfly shape, due to the well-known ferroelectric hysteresis. At the bias electric field of 100 kV/cm, the relative permittivity of ≈ 650 render to tunability of $\approx 46\%$, defined as $[\varepsilon(0) - \varepsilon(v)] / \varepsilon(0) \times 100\%$. The value of tunability is anticipated higher at a lower density of misfit dislocations by reducing the lattice mismatch of 5.03% between PLZT and LNO, for example, selection of a different bottom electrode, since misfit dislocations can pin the dipoles and make switching difficult under high electric field and broader peaks.^{26–28} It is found that the relative permittivity decreases with frequency,

following the logarithmic relationship in the frequency range of 100 Hz–100 kHz, as shown in Fig. 3(b). In contrast, the dielectric loss is independent of frequency at lower frequencies below ~ 10 kHz, followed by monotonic increases with frequency at higher frequencies. These typical dielectric dispersion trends in the parallel plate capacitor testing configuration are result from space charge relaxation, namely, the Maxwell-Wagner relaxation caused by space charge polarization at the ferroelectric film/electrode interface.

The ferroelectric properties of the samples were further confirmed in the nested P-E hysteresis loops, as shown in Fig. 4(a). While this behavior in epitaxial PLZT films is qualitatively similar to that of the polycrystalline PLZT ones, the coercive field (E_c) in the former is much smaller than that of their polycrystalline counterparts. For example, E_c is 21 kV/cm under the applied field of 150 kV/cm in the former, about 4 kV/cm lower than in the latter, indicating that it is easier to electrically switch and domain wall pinning is reduced in epitaxial PLZT films.²⁹ The reduced domain wall pinning is probably resulting from the reduced number of grain boundaries, which is a key factor to obstruct the movement of the ferroelectric domains.³⁰ As shown in Figure 4(b), the E_c and P_r both increase with increasing maximum applied field (E_{max}) due to the fact that a larger applied field leads to increased domain wall movement and better electrical dipole alignment in the samples.

The reduced defect density in epitaxial ferroelectric films is expected to correlate directly to their nonlinearity. In order to quantify it, nonlinear dielectric response of the epitaxial PLZT films was examined in comparison with their polycrystalline counterparts. Fig. 5(a) depicts the dielectric permittivity change with frequency between 200 Hz and 100 kHz. The measurements were conducted with a small oscillation signal ($E = E_0 \sin \omega t$) of various amplitude E_0 . The real permittivity

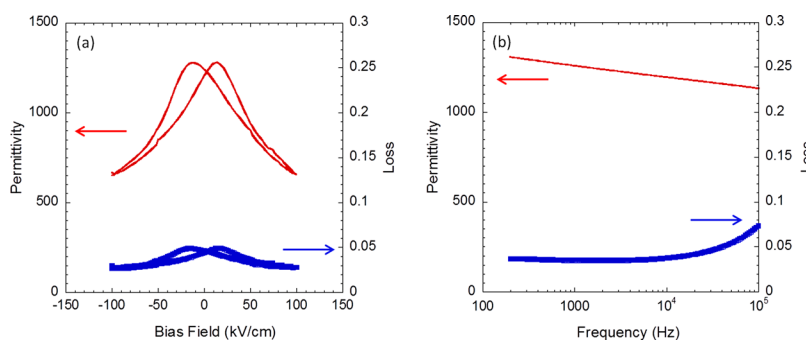


FIG. 3. Dielectric property as a function of (a) bias field, (b) frequency in epitaxial PLZT films.

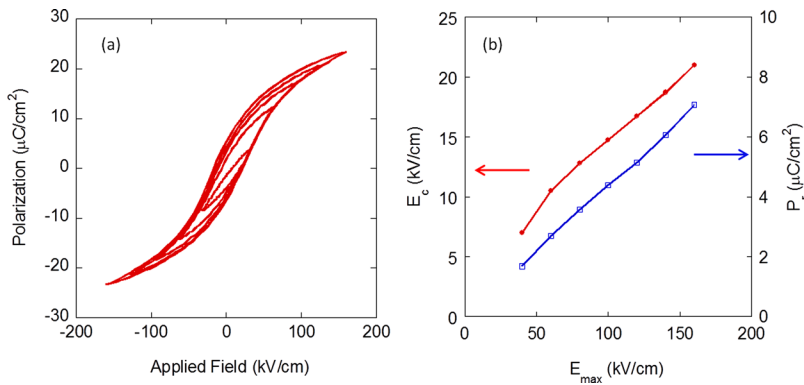


FIG. 4. (a) P-E hysteresis loops and (b) coercive field and remnant polarization vs E_{\max} in epitaxial PLZT films.

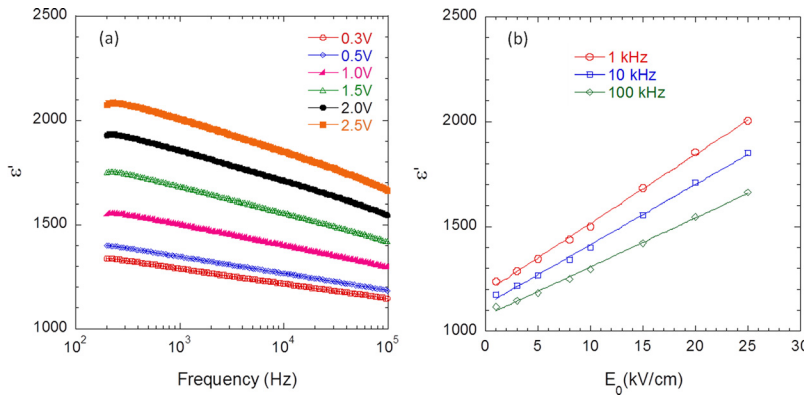


FIG. 5. Frequency dependent dielectric permittivity change with (a) frequency and (b) ac signal amplitude in epitaxial PLZT films.

ε' increases with the increasing ac field amplitude E_0 but decreases with the increasing frequency. The linear dependence of ε' on the logarithm of frequency indicates that the extrinsic factors, such as motions of charged defect species and domain walls, are the contributing factors to the polarization under low applied ac field. To quantitatively assess the contribution of the extrinsic effect on permittivity, we plotted ε' as a function of E_0 in Fig. 5(b) and the data fit well to the Rayleigh law (solid lines):³¹ $\varepsilon' = \varepsilon'_{init} + \alpha' \times E_0$, where ε'_{init} and α' are initial (zero field) permittivity and irreversible Rayleigh coefficient, respectively. The ε'_{init} is from the intrinsic lattice polarizability and reversible domain wall motion. α' originates from the irreversible motion of domain wall and is proportional to the concentration of pinning centers inversely. It should be noted that at ac field $E_0 = 25$ kV/cm, the irreversible extrinsic contribution in the epitaxial film contributes around 50% of the total dielectric response at 1 kHz, which is twice larger than PZT (45/55) films. The corresponding Rayleigh parameters derived from least square fitting of the experimental data are summarized in Table I. The $\alpha'/\varepsilon'_{init}$ ratio is a normalized parameter and an excellent quantitative tool to measure the extrinsic contributions to dielectric properties of a ferroelectrics. The dielectric nonlinearity

can go up to 0.028 cm/kV at 1 kHz, which is twice as much higher than those reported for polycrystalline PZT (52/48) and PLZT.^{29,32} The higher nonlinearity is likely due to reduced pinning centers in the epitaxial PLZT films, inducing that mobility of the domain wall, the extrinsic contribution to the dielectric property, is higher than the polycrystalline film. While the ratio of irreversible Rayleigh parameter to reversible parameter decreases monotonically with increasing frequency, from 0.028 cm/kV at 1 kHz to 0.022 cm/kV at 100 kHz, a much less dependence on frequency was observed in epitaxial PLZT films as compared to their polycrystalline counterparts.²⁹ This observation is very important in confirming higher mobility of the available interfaces or a higher concentration of mobile interfaces in epitaxial PLZT films.

In summary, high quality epitaxial PLZT/LNO heterostructures were obtained on LAO substrate by using PLD. The primary benefit of the epitaxy is in reducing the concentration of growth defects, in particular the large-angle grain boundaries so as to enhance the electric dipole mobility. The relative permittivity is above 1200 and dielectric loss is as low as 4% under zero bias. The tunability at 100 kV/cm is as high as 46%. The ratio of irreversible/extrinsic and reversible/intrinsic dielectric responses exhibits less dependence on frequency and is twice higher than that of the polycrystalline PLZT films, indicating that the epitaxial PLZT films indeed have a lower defect concentration and reduced domain pinning, resulting in enhanced dielectric properties.

The authors acknowledge support in part by NASA Contract No. NNX13AD42A, ARO Contract No. ARO-W911NF-12-1-0412, and NSF Contract Nos. NSF-DMR-1105986 and NSF EPSCoR-0903806, and matching support

TABLE I. Rayleigh parameter of the epitaxial PLZT film.

Frequency (kHz)	α' (cm/kV)	ε'_{init}	$\alpha'/\varepsilon'_{init}$ (cm/kV)
1	32.77 ± 0.58	1187.6 ± 7.6	0.028
10	28.67 ± 0.54	1127.2 ± 7.3	0.025
100	23.34 ± 0.51	1074 ± 6.8	0.022

from the State of Kansas through Kansas Technology Enterprise Corporation. Work at Argonne was funded by the U.S. Department of Energy, Vehicle Technologies Program, under Contract No. DE-AC02-06CH11357. The work also was funded by the National Science Foundation of China under Grant No. NSFC-51202185 and 51390472.

- ¹Y. Lin, X. Chen, S. W. Liu, C. L. Chen, J. S. Lee, Y. Li, Q. X. Jia, and A. Bhalla, *Appl. Phys. Lett.* **84**, 577 (2004).
- ²C. L. Jia, K. W. Urban, M. Alexe, D. Hesse, and I. Vrejoiu, *Science* **331**, 1420 (2011).
- ³R. Ramesh, A. Inam, W. K. Chan, F. Tillerot, B. Wilkens, C. C. Chang, T. Sands, J. M. Tarascon, and V. G. Keramidas, *Appl. Phys. Lett.* **59**, 3542 (1991).
- ⁴R. Ramesh, W. K. Chan, B. Wilkens, H. Gilchrist, T. Sands, J. M. Tarascon, V. G. Keramidas, D. K. Fork, J. Lee, and A. Safari, *Appl. Phys. Lett.* **61**, 1537 (1992).
- ⁵C. L. Wu, P. W. Lee, Y. C. Chen, L. Y. Chang, C. H. Chen, C. W. Liang, P. Yu, Q. He, R. Ramesh, and Y. H. Chu, *Phys. Rev. B* **83**, 020103(R) (2011).
- ⁶R. Caruso, O. de Sanctis, A. Frattini, C. Steren, and R. Gil, *Surf. Coat. Technol.* **122**, 44 (1999).
- ⁷Z. J. Wang, Z. P. Cao, Y. Otsuka, N. Yoshikawa, H. Kokawa, and S. Taniguchi, *Appl. Phys. Lett.* **92**, 222905 (2008).
- ⁸S. Y. Liu, L. Chua, K. C. Tan, and S. E. Valavan, *Thin Solid Films* **518**, E152 (2010).
- ⁹M. Tyunina, J. Levoska, A. Sternberg, and S. Leppavuori, *J. Appl. Phys.* **84**, 6800 (1998).
- ¹⁰B. Yang, T. K. Song, S. Aggarwal, and R. Ramesh, *Appl. Phys. Lett.* **71**, 3578 (1997).
- ¹¹B. H. Ma, S. Chao, M. Narayanan, S. S. Liu, S. Tong, R. E. Koritala, and U. Balachandran, *J. Mater. Sci.* **48**, 1180 (2013).
- ¹²B. H. Ma, D. K. Kwon, M. Narayanan, and U. Balachandran, *J. Electroceram.* **22**, 383 (2009).
- ¹³M. Narayanan, U. Balachandran, S. Stoupin, B. H. Ma, S. Tong, S. Chao, and S. S. Liu, *J. Phys. D-Appl. Phys.* **45**, 335401 (2012).
- ¹⁴S. Tong, B. H. Ma, M. Narayanan, S. S. Liu, R. Koritala, U. Balachandran, and D. L. Shi, *ACS Appl. Mater. Interfaces* **5**, 1474 (2013).
- ¹⁵F. Xu, S. Trolrier-McKinstry, W. Ren, B. M. Xu, Z. L. Xie, and K. J. Hemker, *J. Appl. Phys.* **89**, 1336 (2001).
- ¹⁶H. F. Cheng, *J. Appl. Phys.* **78**, 4633 (1995).
- ¹⁷T. F. Tseng, K. S. Liu, T. B. Wu, and I. N. Lin, *Appl. Phys. Lett.* **68**, 2505 (1996).
- ¹⁸M. Gaidi, A. Amassian, M. Chaker, M. Kulishov, and L. Martinu, *Appl. Surf. Sci.* **226**, 347 (2004).
- ¹⁹X. X. Guo, C. L. Li, Y. L. Zhou, and Z. H. Chen, *J. Vac. Sci. Technol. A* **17**, 917 (1999).
- ²⁰R. N. P. Choudhary and J. Mal, *Mater. Lett.* **54**, 175 (2002).
- ²¹S. Sriram, M. Bhaskaran, D. R. G. Mitchell, K. T. Short, A. S. Holland, and A. Mitchell, *Microsc. Microanal.* **15**, 30 (2009).
- ²²A. Gruverman, O. Auciello, and H. Tokumoto, *Annu. Rev. Mater. Sci.* **28**, 101 (1998).
- ²³K. Jonscher, *Dielectric Relaxation in Solids*, 1st ed. (Chelsea Dielectrics Press, London, 1983).
- ²⁴B. H. Ma, D. K. Kwon, M. Narayanan, and U. Balachandran, *J. Phys. D-Appl. Phys.* **41**, 205003 (2008).
- ²⁵M. Lallart, *Ferroelectrics - Physical Effects* (InTech, 2011), pp. 106–107.
- ²⁶B. H. Ma, S. S. Liu, S. Tong, M. Narayanan, R. E. Koritala, Z. Q. Hu, and U. Balachandran, *Smart Mater. Struct.* **22**, 055019 (2013).
- ²⁷B. H. Ma, S. S. Liu, S. Tong, M. Narayanan, and U. Balachandran, *J. Appl. Phys.* **112**, 114117 (2012).
- ²⁸Z. G. Ban and S. P. Alpay, *J. Appl. Phys.* **93**, 504 (2003).
- ²⁹B. H. Ma, Z. Q. Hu, S. S. Liu, M. Narayanan, and U. Balachandran, *Appl. Phys. Lett.* **102**, 072901 (2013).
- ³⁰M. V. Raymond, J. Chen, and D. M. Smyth, *Integr. Ferroelectr.* **5**, 73 (1994).
- ³¹D. Damjanovic and M. Demartin, *J. Phys. D-Appl. Phys.* **29**, 2057 (1996).
- ³²P. Bintachitt, S. Jesse, D. Damjanovic, Y. Han, I. M. Reaney, S. Trolrier-McKinstry, and S. V. Kalinin, *Proc. Natl. Acad. Sci. U.S.A.* **107**, 7219 (2010).